開窓器を用いるなどしてアプローチを工夫することで、展開時の筋肉の切離や骨切除の量を最小限にする形での手術の施行が可能になり、手術後のリハビリテーションの進行を促進することが出来ると考えられた。

E. 結論

脊髄損傷後、SI投与とリハビリテーションの併用により再生軸索のrewiringが促進され、運動機能改善促進効果が得られた。本研究結果より、損傷後早期の適切なリハビリテーションの併用が再生軸索のrewiring促進効果を有する可能性が示唆された。

F. 健康危険情報

特になし

G. 研究発表(2014年度)(主要分)

1.論文発表

(英語論文)

Cao K, Watanabe K, Hosogane N, Toyama Y, Yonezawa I, Machida M, Yagi M, Kaneko S, Kawakami N, Tsuji T, Matsumoto M:
Association of postoperative shoulder balance with adding-on in Lenke Type II adolescent idiopathic scoliosis.
Spine(Phila Pa 1976), 39(12): E705-712 (2014.5.20)

Kondo T, Funayama M, Tsukita K, Hotta A, Yasuda A, Nori S, Kaneko S, Nakamura M, Takahashi R, Okano H, Yamanaka S, Inoue H:
Focal Transplantation of Human iPSC-Derived Glial-Rich Neural Progenitors Improves Lifespan of ALS Mice.
Stem Cell Reports, 3(2): 242-249 (2014.8.12)

Satoh S, Yagi M, Machida M, Yasuda A, Konomi T, Miyake A, Fujiyoshi K, Kaneko S, Takemitsu M, Machida M, Yato Y, Asazuma T:
Reoperation rate and risk factors of elective spinal surgery for degenerative spondylolisthesis —minimum 5 year follow-up—
The Spine Journal: e25681581 (2015.2.11)

Hosogane N, Watanabe K, Yagi M, Kaneko S, Toyama Y, Matsumoto M:
Scoliosis is a Risk Factor for Gastroesophageal Reflux Disease in Adult Spinal Deformity
Journal of Spinal Disorders & Techniques: e25789717 (2015.3.18)

(日本語論文)

朝妻孝仁, 金子慎二郎:
感染症診療 update II章 主要な臓器感染症 J. 骨・関節感染症 椎間板炎, 椎体炎
日本医師会雑誌, 143 特別号(2): S183-185 (2014.10.15)

金子慎二郎, 許斐恒彦, 谷戸祥之, 朝妻孝仁:
成人脊柱変形に対する手術前simulationとしてのcasting testの有効性
Monthly Book Orthopaedics, 28(2): 23-29, 2015

2.学会発表

Shinjiro Kaneko, Masaya Nakamura, Hitoshi Kono, Yoshiyuki Yato, Yoshiaki Toyama, Morio Matsumoto and Takashi Asazuma:
Atlanto-occipital subluxation: report of an atypical case and review of the literature
5th Annual Meeting of Cervical Spine Research Society Asia Pacific Section, Viet Nam (2014.4.3-5)

金子慎二郎, 谷戸祥之, 町田正文, 竹光正和, 八木満, 藤吉兼浩, 三宅敦, 許斐恒彦, 安田明正, 佐藤俊輔, 朝妻孝仁:
近傍椎体に既存(陳旧性)骨折を有する骨粗鬆症性椎体圧潰に対する前方固定術
第43回日本脊椎脊髄病学会学術集会、京都 (2014.4.17-19)

金子慎二郎, 河野仁, 齊藤正史, 谷戸祥之, 朝妻孝仁:
Atlanto-occipital subluxation(AOS)の新規分類法の提唱とO-C1角の標準値に関する解析
第43回日本脊椎脊髄病学会学術集会、京都 (2014.4.17-19)

金子慎二郎, 谷戸祥之, 町田正文, 竹光正和, 八木満, 藤吉兼浩, 三宅敦, 許斐恒彦, 安田明正, 佐藤俊輔, 朝妻孝仁:
結核性脊椎炎に対する前方固定術による後弯変形矯正に関する検討と後方instrumentation追加の際の工夫(CBT法の応用)
第43回日本脊椎脊髄病学会学術集会、京都 (2014.4.17-19)

金子慎二郎, 齊藤正史, 河野仁, 許斐恒彦, 安田明正, 谷戸祥之, 朝妻孝仁:

成人脊柱変形に対する手術前 simulation としての casting test の有効性と test 法の普遍性に関する検討
第 23 回日本脊椎インストゥルメンテーション学会、浜松(2014.8.29-30)

金子慎二郎, 齊藤正史, 河野仁, 渡邉泰伸, 中道清広, 谷戸祥之, 朝妻孝仁:
成人脊柱変形に対する矯正固定術前後の全脊柱 alignment の代償性変化に関する検討―非固定椎での矢状面 alignment 変化を中心として―
第 23 回日本脊椎インストゥルメンテーション学会、浜松(2014.8.29-30)

金子慎二郎, 齊藤正史, 河野仁, 渡邉泰伸, 中道清広, 許斐恒彦, 谷戸祥之, 朝妻孝仁:
成人脊柱変形に対する後方矯正固定術前後の非固定椎での代償性 alignment 変化とその手術前に於ける予想手段に関する検討
第 48 回日本側彎症学会学術集会、盛岡(2014.10.30-11.1)

金子慎二郎, 白井雅人, 許斐恒彦, 谷戸祥之, 朝妻孝仁:
腰椎側方アプローチに於ける腎臓の位置関係に関する検討
第 1 回日本脊椎前方側方進入手術研究会、東京(2015.2.1)

金子慎二郎, 齊藤正史, 河野仁, 渡邉泰伸, 中道清広, 許斐恒彦, 谷戸祥之, 朝妻孝仁:
成人脊柱変形に対する後方矯正固定術前後の非固定椎での代償性 alignment 変化とその術前予想手段に関する検討
第 5 回日本成人脊柱変形学会、東京(2015.3.8)

金子慎二郎, 谷戸祥之, 朝妻孝仁:
脊椎カリエスに対する治療のアルゴリズム
第 90 回日本結核病学会総会、長崎(2015.3.27-28)

金子慎二郎:
成人脊柱変形と腰椎変性疾患に対する手術に於ける OLIF の応用
第 31 回多摩脊椎脊髄カンファレンス、東京(2014.6.5)

金子慎二郎:
成人脊柱変形に対する手術に於ける OLIF の応用
第 2 回中部 MISt 研究会、名古屋(2014.9.6)

金子慎二郎:
成人脊柱変形に対する手術に於ける OLIF の応用
第 1 回 OLIF セミナー、東京(2015.1.31)

金子慎二郎:
胸腰椎前方手術手技・合併症(日本整形外科学会教育研修講演)
第 1 回日本脊椎前方側方進入手術研究会、東京(2015.2.1)

H. 知的財産権の出願・登録状況
1. 特許取得
特になし
2. 実用新案登録
特になし
3. その他
特になし

厚生労働科学研究費補助金
(障害者対策総合研究事業（障害者対策総合研究開発事業（身体・知的等障害分野）))
分担研究報告書

脊髄損傷の個別診断による歩行訓練法選択の最適化に関する研究
がん脊椎転移による脊髄損傷の MRI 定量的評価法の開発

研究分担者　住谷　昌彦　東京大学医学部附属病院緩和ケア診療部　准教授

研究要旨

がん脊椎転移では脊髄圧迫による脊髄損傷を引き起こし、四肢運動麻痺や膀胱直腸障害、痛みなどで患者の ADL および QOL は大きく低下することがある。しかし、がん脊椎転移では必ずしも脊髄損傷を発症する訳では無く、さらに、がんによる全身状態の悪化も相まって侵襲的治療よりも保存的治療法が選択されることが多いのが実情である。そこで、がん脊椎転移患者のうち脊髄損傷を続発しやすい高リスク患者を選択し積極的治療介入を実現するために、がん脊椎転移による脊髄損傷患者の MRI 定量的評価法を開発することを目的とした。がん脊椎転移患者 15 名の MRI axial 断面のべ 66 画像を脊椎前方成分（椎体）と後方成分（脊柱管と椎弓根と棘突起）に分離し、前方成分および後方成分を脊椎テンプレートに合致するように左右・前後径を拡大・縮小し、その修正画像上のがん部位の輪郭を脊椎テンプレート上に描画した。これを、下肢筋力低下（徒手筋力評価 3 以下、3 以上）の 2 群と膀胱直腸障害の有無の 2 群に比較し、それぞれの群におけるがん位置を比較した。その結果、下肢筋力低下患者では椎体後方にがんが存在し脊柱管前方から脊髄を圧迫していること、膀胱直腸障害患者では椎体後方にがんが存在し脊柱管前方から脊髄を圧迫していることに加えて椎弓にもがんが存在し脊髄を外側方から圧迫していることが明らかになった。したがって、これらの位置にがんが転移している場合には将来的に運動麻痺や膀胱直腸障害を生じる可能性があるため積極的な侵襲治療の適応を考慮する必要があることを示唆する。将来的な治療介入の適応判断のために、がん脊椎転移による脊髄損傷の MRI 定量的評価法の開発は有用であると考えられる。

A．研究目的

本邦の新規がん患者は年間 80 万人と推計され、継続的にがん治療中の患者は 200 万人と推計されている。これら担癌患者のうち約 20-36%はがん脊椎転移を発症し、その頻度は胸椎 66%、腰椎 22%、頚椎 11%とされ、10-23%はがん脊椎転移による痛みなどの症状を有し、5-10%は脊髄損傷を発症する。

脊髄損傷では、求心路遮断による神経障害性疼痛が発症し、患者の生活の質(Quality of Life ：QOL)が大きく損なわれる。さらに、疼痛だけでなく運動麻痺と痙性などの不随意運動による運動障害が日常生活動作(Activities of daily living ：ADL)を低下させる。このような脊髄損傷を引き起こす原因は、これまでは外傷が大半であったが、人口の高齢化に伴ってがん患者が増加し、さらにがん脊椎転移による脊髄損傷が増加してきているのが実情である。がん脊椎転移に対する治療法は、放射線療法や整形外科的脊椎固定術、化学療法に加えて、最近はバルーン椎体形成術

などの新しい低侵襲治療も実施されているが骨粗鬆症性脊椎圧迫骨折に対する施術よりも合併症が比較的多いことが問題点として報告されている。がん脊椎転移による脊髄損傷が起こった場合には、脊髄の早期除圧が必要であるため最も治療効果が期待できる方法は脊椎固定術であるが、がん患者の全身状態の悪化や、脊椎転移は 86.3%が複数の脊椎に及ぶため手術適応の幅が狭く、時間的治療効果は劣るが侵襲度が低く適応が比較的広い放射線療法が選択されることが多い。しかしながら、放射線療法では治療効果が発現するのに最低 2 週間程度を要するため、腫瘍が縮小し脊髄の除圧が得られた際には脊髄損傷が不可逆的に完成してしまっている例も少なくない。

そこで本研究では、がん脊椎転移の画像診断的特徴から運動麻痺や膀胱直腸障害を発現する頻度が高い評価方を開発し、治療介入の適応判断の基盤とすることを目標にする。

B．研究方法

対象は 2012 年 2 月から 2013 年 2 月にかけて東京大学医学部附属病院脊髄損傷ボードで診療したがん脊椎転移患者 15 名。徒手筋力テストで 3 以下の筋力低下を伴う患者は 10 名で、膀胱直腸障害を伴う患者は 8 名であった。脊椎転移部位の MRI 画像診断を後方視的に解析した。研究の実施にあたっては、東京大学医学部倫理委員会による承認を得た。

がん脊椎転移が認められる椎骨の MRI axial 像について、脊椎前方成分（椎体）と後方成分（脊柱管、椎弓根、棘突起）に分離し、前方成分および後方成分を脊椎テンプレートに合致するように左右・前後径を拡大・縮小した。その修正画像上の転移がんの輪郭を手作業で脊椎テンプレート上に描画した。各患者のがん転移がある脊椎全てに同様の作業を行った。この作業の後に、患者群を A）と集金力テスト 3 以下ないしは 3 より大きい 2 群に分類、B）膀胱直腸障害の有無で 2 群に分類、C)がん転移脊椎の圧迫骨折の膿むで 2 群に分類の 3 条件について、脊椎テンプレート上に重ねて描画された転移がんの位置を比較した。

C．研究結果

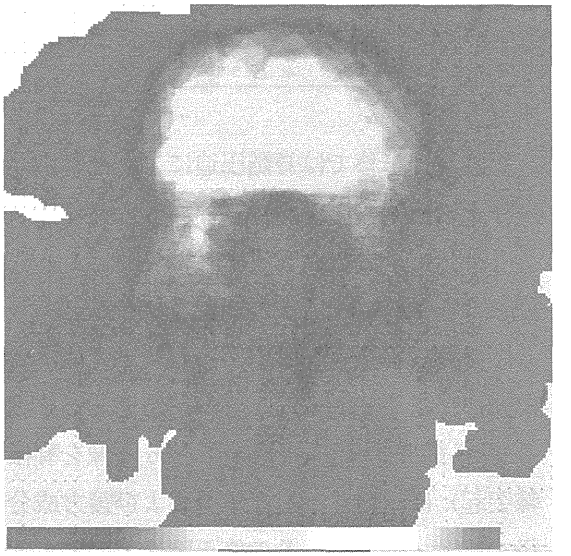

図 1 がん脊椎転移患者 15 名、のべ 66MRI axial 像における転移がんの位置

椎体へのがん転移が最も多く、続いて椎弓根へとがんが連続性を持って転移していることが示された。横突起や棘突起へのがん転移は少ないことが明らかになった。

図2-1 徒手筋力テスト3以下のがん脊椎転移患者の MRI axial 像における転移がんの位置

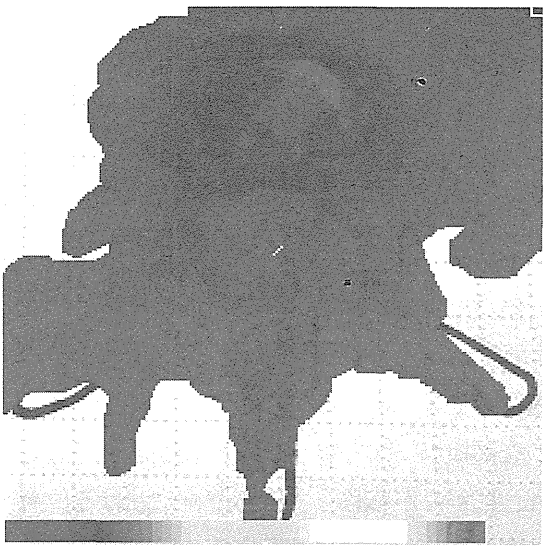

図2-2 徒手筋力テスト3より大きいがん脊椎転移患者のMRI axial像における転移がんの位置

下肢筋力低下を伴うがん脊椎転移患者では、椎体の後方部へのがん転移が顕著であった。

図 3-1 膀胱直腸障害を伴うがん脊椎転移患者のMRI axial像における転移がんの位置

図 3-2 膀胱直腸障害を伴わないがん脊椎転移患者のMRI axial像における転移がんの位置

膀胱直腸障害を伴うがん脊椎転移患者では、椎体後方だけでなく、椎弓根部へのがん転移も明確であった。

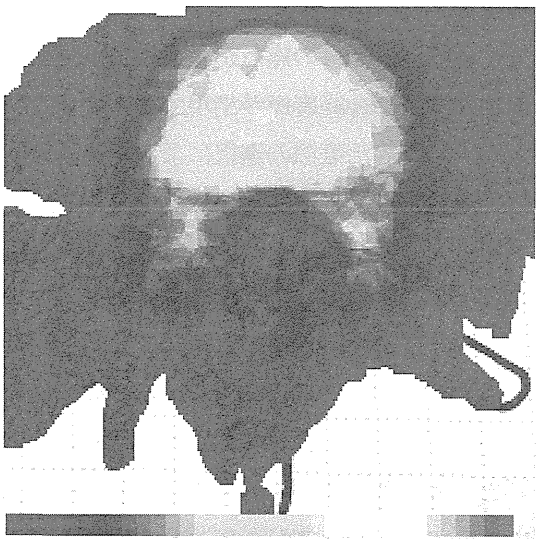

図 4-1 脊椎圧迫骨折を伴うがん脊椎転移患者のMRI axial像における転移がんの位置

図 4-2 脊椎圧迫骨折を伴わないがん脊椎転移患者のMRI axial像における転移がんの位置

椎体の圧迫骨折を伴う患者では、椎体の中心部に焦点を持つがん転移があり、圧迫骨折を伴わない患者では椎体後方に焦点があった。

D. 考察

がん脊椎転移による脊髄損傷時の下肢運動麻痺は脊髄前部を下行する前皮質脊髄路あるいは脊髄前角運動神経細胞あるいは神経根前枝のいずれの障害によっても起こり得る。下肢麻痺を呈した脊髄損傷患者では、椎体後方に転移がんの焦点があり、これら神経細胞・神経線維・神経路の障害を示唆する。したがって、脊椎がん転移の焦点が椎体後方部にある場合には運動神経麻痺が出現する可能性を考慮し、侵襲的治療法の選択による即時的な脊髄圧迫の解除が必要となる可能性が高い。

脊髄を介した膀胱支配は、脳幹橋部から腰髄前角への下行性の運動経路と脊髄外側を上行する感覚経路が左右に1本ずつ計4本の神経路によって支配されている。膀胱直腸障害を呈した脊髄損傷患者の転移がんの焦点は、脊髄前角を障害していると考えられる椎体後方に加えて、脊髄外側から圧迫していると考えられる椎弓根部にもがん転移が認められた。この画像所見は、脊髄損傷時の膀胱直腸障害の出現は、下行性運動路と上行性感覚路の両方の障害の場合に出現しやすいとされるこれまでの知見に合致する。したがって、椎体後方のがん転移だけでなく椎弓根部にもがん転移がある場合にも積極的な早期治療が必要であると考えられる。

がん脊椎転移による圧迫骨折では、円背による仰臥位困難などから安静臥床が取りづらく睡眠障害などに直結することで患者のQOLを低下させる。椎体の中心部のがん転移では圧迫骨折をきたしやすいことが画像所見の特徴からは示されており、バルーン椎体形成術などの適応を検討する際の参考になるものと思われる。

このような画像所見の評価方法から、上記の位置にがんが転移している場合には将来的に運動麻痺や膀胱直腸障害を生じる可能性があるため積極的な侵襲治療の適応を考慮する必要があることを示唆する。将来的な治療介入の適応判断のために、がん脊椎転移による脊髄損傷のMRI定量的評価法の開発は有用であると考えられる。

E．結論

がん脊椎転移による脊髄損傷の発生に関連した転移がんの位置をMRIで評価する方法を開発した。この評価方法からがん脊椎転移後の脊髄損傷による症状予測に繋がると考えられ、にがんが転移している脊椎における位置に応じて、将来的に運動麻痺や膀胱直腸障害を生じる可能性があるため積極的な侵襲治療の適応を考慮する際に有用であると考えられる。

F．健康危険情報

なし

G．研究発表

1.論文発表

Sumitani M,..,Ogata T, et al. Dissociation in accessing space and number representation in pathologic pain patients. Brain Cogn 2014; 90: 151-6

住谷昌彦，緒方徹，竹下克志．神経障害性疼痛の概念と臨床評価．東京都医師会雑誌 2014; 67: 17-23

住谷昌彦，緒方徹．神経リハビリテーション治療．脳21 2014; 17: 238-43

住谷昌彦，熊谷晋一郎，緒方徹，宮内哲．難治性疼痛に対する神経リハビリテーション ペインクリニック 2014;35: S265-76

住谷昌彦，緒方徹．脊髄刺激療法の鎮痛機序．痛みの Science&Practice:神経ブロックに必要な画像解剖．編集：表圭一，文光堂 p292-3, 2014

H．知的財産権の出願・登録状況（予定を含む。）

1. 特許取得

なし

2. 実用新案登録

なし

3. その他

なし

厚生労働科学研究費補助金
（障害者対策総合研究事業（障害者対策総合研究開発事業（身体・知的等障害分野））

神経損傷バイオマーカー開発に関する研究

研究分担者　　山内　淳司　　国立成育医療研究センター研究所　室長

研究要旨
近年、神経科学領域で注目されている脊髄可塑性の科学的根拠に立脚した神経リハビリテーション（neurorehabilitation）方法の体系化において、適応症例の選別法についての基礎基盤構築を目指す。当該班研究においてすでに臨床データが蓄積されつつある軸索損傷マーカーの pNF-H は今後様々な疾患において臨床情報を補完する血液マーカーとして期待されるが、その血中上昇メカニズムは必ずしも明らかではない。
本年度は pNF-H 上昇のメカニズムを解析する為に培養系の神経損傷モデルを作成し、pNF-H の漏出メカニズムについて検討を行った。得られた結果からは軸索の損傷形態が pNF-H の放出に影響を及ぼすというもので、損傷によって障害された軸索のセグメントが pNF-H のオリジンである可能性が示唆された。こうした pNF-H に関する基礎知見が増していくことで、今後、この新規のマーカー値を正しく判断することが可能となり、脊髄損傷のみならず、他の神経疾患においても疾患の診断や重症度評価に寄与することが期待される。

A．研究目的

当該研究班でもすでに取り上げている軸索伸長バイオマーカーPNF-Hは神経損傷に伴って末梢血液・脳脊髄液中に漏出することが報告されており、すでに脊髄損傷臨床例での調査が実施されている。

こうした臨床面での展開とはうらはらに、本来神経細胞（ニューロン）の細胞内で発現しているｐNF-H がどの様な経路とメカニズムで血中あるいは脳脊髄液中に達するかの知見はごく限られている。新規のマーカーを臨床に利用する場合、その値の変動が意味する生命現象を理解することは、値の解釈において重要であることは言うまでもない。特に、血中pNF-H値は他の神経損傷マーカー（たとえばS100B）が一過性の上昇を示し、数日内に正常化するのと異なり、数週間から数か月にわたって上昇・高値維持を示すことが特徴として挙げられる。こうした変化が何を示すのか、また治療介入による変化を捉える指標となりうるのかが分かることによってpNF-Hはさらに有用性の高いマーカーになることが期待される。

こうした目的のもと、本年度は培養系における神経損傷実験系を立ち上げ、その中での培養液中へのpNF-H漏出を検出することでそのメカニズムを検討した。

B．研究方法

1）培養神経細胞損傷モデルの作成

神経細胞として損傷可能な長い軸索を豊富に伸ばす、後根神経節を選択し、ラットの胎生15日目よりこれを採取した。後根神経節は採取後そのままの形でコラーゲンコートしたプラスチック・ディスク上に播種され、その後3週間培養し、約1cm程度の軸索がディスク上に形成されるまで、NGF存在下で培養を行った。

2）神経損傷の作成

神経損傷はメスまたは鈍的に軸索を切断する。損傷翌日、メディウムを採取し、中に含まれるpNF-HをELISA法によって測定した。神経の切断においては、軸索のみを切断する方法と、ディスクごと切離する方法を実施した。ディスクごと切り離した場合は、切断から遠位側と近位（細胞体）側とを分離して培養する実験も行った。

C．研究結果

培養条件での軸索損傷においてもpNF-Hの放出は観察された。そして、その値からは神経損傷の方法によって、pNF-Hの放出に差異が生じる可能性が示唆された。

具体的には、比較的鋭的に切れたばあいよりも挫滅が強く生じるようにして軸索を切った場合の方がpNf-Hの放出量が高い傾向が見られた。

D．考察

pNf-Hの血中上昇機序については不明な点が多く残されており、このマーカーを臨床的に用いる上での障壁となっている。

これまでpNF-Hの放出メカニズムとして、損傷部より遠位部がワーラー変性を起こす過程で骨格蛋白が漏出するメカニズムと、損傷後も細胞体からpNF-Hの輸送が続き、これが漏出するメカニズムとが想定されていた。しかし、今回の結果は損傷の近位部から、あるいは遠位部からという区別ではなく、損傷部そのものの状態がpNf-Hの値に影響するというものであった。可能性として、放出されるpNF-Hは損傷部周辺の軸索が変性する過程で生じ、損傷部が広い範囲に広がる挫滅型では変性も広範囲で起きるためpNF-Hの上昇も高度である、という可能性である。

E．結論

本研究の結果からはpNF-Hの上昇メカニズムについて確定的なモデルを提唱することは困難である。今後、より定量性の優れたモデル解析を行うことで、

そのメカニズムがより明確になることが期待される。また、動物実験においてもpNF-Hの血中半減期などからのアプローチも考えられる。

pNF-H放出のメカニズムを明確にすることは、今後のバイオマーカーとしての利用と解釈の上で重要な知見になると考えられる。

F. 健康危険情報

特になし

G. 研究発表

1. 論文発表

1. Miyamoto Y, Torii T, Eguchi T, Nakamura K, Tanoue A, Yamauchi J, Hypomyelinating leukodystrophy-associated missense mutant of FAM126A/hyccin/DRCTNNB1A aggregates in the endoplasmic reticulum. J Clin Neurosci 2014 21(6):1033-1039

2. Miyamoto Y, Yamamori N, Torii T, Tanoue A, Yamauchi J, Rab35, acting through ACAP2 switching off Arf6, negatively regulates oligodendrocyte differentiation and myelination. Mol Biol Cell 2014 25(9):1532-1542

3. Torii T, Miyamoto Y, Yamauchi J, Tanoue A, Pelizaeus-Merzbacher disease: cellular pathogenesis and pharmacologic therapy. Pediatr Int 2014 56(5):659-666

4. Torii T, Miyamoto Y, Takada S, Tsumura H, Arai M, Nakamura K, Ohbuchi K, Yamamoto M, Tanoue A, Yamauchi J, In vivo knockdown of ErbB3 in mice inhibits Schwann cell precursor migration. Biochem Biophys Res Commun 2014 452(3):782-788

5. Torii T, Miyamoto Y, Tago K, Sango K, Nakamura K, Sanbe A, Tanoue A, Yamauchi J, Arf6 Guanine Nucleotide Exchange Factor Cytohesin-2 Binds to CCDC120 and Is Transported Along Neurites to Mediate Neurite Growth. J Biol Chem 2014 289(49):33887-38903

2. 学会発表

特になし

F. 知的財産権の出願・登録状況

1. 特許取得

特になし

2. 実用新案登録

特になし

3. その他

研究成果の刊行に関する一覧表

書籍

著者氏名	論文タイトル名	書籍全体の編集者名	書　籍　名	出版社名	出版地	出版年	ページ

雑誌

発表者氏名	論文タイトル名	発表誌名	巻号	ページ	出版年
Tazoe T, Endoh T, Kitamura T, Ogata T,	Polarity specific effects of transcranial direct current stimulation on interhemispheric inhibition	PLoS One	9(12)	e114244	2014
Masugi Y, Kitamura T, Kamibayashi K, Ogawa T, Ogata T, Kawashima N, Nakazawa K	Velocity-dependent suppression of the soleus H-reflex during robot-assisted passive stepping	Neurosci Lett,	584	337-41	2015
Natori A, Ogata T, Sumitani M, Kogure T, Yamauchi T, Yamauchi H	Potential role of pNF-H, a biomarker of axonal damage in the central nervous system, as a predictive marker of chemotherapy-induced cognitive impairment	Clinical Cancer Research	21(6)	1348-52	2015
Yaeshima K, Negishi D, Yamamoto S, Ogata T, Nakazawa K, Kawashima N.	Mechanical and neural changes in plantar-flexor muscles after spinal cord injury in humans	Spinal Cord	E-publish	1-8	2015
Sumitani M, Ueda H, Hozumi J, Inoue R, Kogure T, Ogata T, Yamada Y.	Minocycline does not decrease intensity of neuropathic pain, but improves its affective dimension.	Journal of Pain & Palliative Care Pharmacotherapy	Early online	1-6	2015

研究成果の刊行物

PLOS | ONE

RESEARCH ARTICLE

Polarity Specific Effects of Transcranial Direct Current Stimulation on Interhemispheric Inhibition

Toshiki Tazoe[1,2*¤], Takashi Endoh[1,3], Taku Kitamura[1,4], Toru Ogata[1]

1. Department of Rehabilitation for Movement Functions, Research Institute, National Rehabilitation Center for Persons with Disabilities, Tokorozawa, Japan, **2.** Japan Society for the Promotion of Science, Tokyo, Japan, **3.** Faculty of Child Development and Education, Uekusa Gakuen University, Chiba, Japan, **4.** Division of Functional Control Systems, Graduate School of Engineering and Science, Shibaura Institute of Technology, Saitama, Japan

*Tot12@pitt.edu

¤ Current address: Systems Neuroscience Institute, Center for the Neural Basis of Cognition, University of Pittsburgh, 4074 BST4, 3501 Fifth Avenue, Pittsburgh, PA, United States of America.

OPEN ACCESS

Citation: Tazoe T, Endoh T, Kitamura T, Ogata T (2014) Polarity Specific Effects of Transcranial Direct Current Stimulation on Interhemispheric Inhibition. PLoS ONE 9(12): e114244. doi:10.1371/journal.pone.0114244

Editor: Nicholas P. Holmes, University of Reading, United Kingdom

Received: July 24, 2014

Accepted: November 5, 2014

Published: December 5, 2014

Data Availability: The authors confirm that all data underlying the findings are fully available without restriction. All relevant data are within the paper.

Funding: This research was supported by Grants-in-Aid for Research Fellow of the Japan Society for the Promotion of Science to TT (#23·10759) and by Grants-in-Aids for Young Scientist B to TE (#24700612). The funders had no role in study design, data collection and analysis, decision to publish, or preparation of the manuscript.

Competing Interests: The authors have declared that no competing interests exist.

Abstract

Transcranial direct current stimulation (tDCS) has been used as a useful interventional brain stimulation technique to improve unilateral upper-limb motor function in healthy humans, as well as in stroke patients. Although tDCS applications are supposed to modify the interhemispheric balance between the motor cortices, the tDCS after-effects on interhemispheric interactions are still poorly understood. To address this issue, we investigated the tDCS after-effects on interhemispheric inhibition (IHI) between the primary motor cortices (M1) in healthy humans. Three types of tDCS electrode montage were tested on separate days; anodal tDCS over the right M1, cathodal tDCS over the left M1, bilateral tDCS with anode over the right M1 and cathode over the left M1. Single-pulse and paired-pulse transcranial magnetic stimulations were given to the left M1 and right M1 before and after tDCS to assess the bilateral corticospinal excitabilities and mutual direction of IHI. Regardless of the electrode montages, corticospinal excitability was increased on the same side of anodal stimulation and decreased on the same side of cathodal stimulation. However, neither unilateral tDCS changed the corticospinal excitability at the unstimulated side. Unilateral anodal tDCS increased IHI from the facilitated side M1 to the unchanged side M1, but it did not change IHI in the other direction. Unilateral cathodal tDCS suppressed IHI both from the inhibited side M1 to the unchanged side M1 and from the unchanged side M1 to the inhibited side M1. Bilateral tDCS increased IHI from the facilitated side M1 to the inhibited side M1 and attenuated IHI in the opposite direction. Sham-tDCS affected neither corticospinal excitability nor IHI. These findings indicate that tDCS produced

polarity-specific after-effects on the interhemispheric interactions between M1 and that those after-effects on interhemispheric interactions were mainly dependent on whether tDCS resulted in the facilitation or inhibition of the M1 sending interhemispheric volleys.

Introduction

Transcranial direct current stimulation (tDCS) is a widely used interventional brain stimulation technique that improves unilateral upper-limb motor function in healthy humans [1–6] and hemiparetic stroke patients [7–11]. Based on the polarity-specific after-effects [12], anodal tDCS is applied to the motor cortex innervating the target limb muscles to enhance corticospinal excitability [5, 8], and cathodal tDCS targets the contralateral motor cortex to suppress the contralateral corticospinal excitability [5, 9], which is assumed to contribute to the reduction of transcallosal inhibition from the contralateral side of the primary motor cortex (M1) to the target M1 side [13, 14]. Based on these strategies, recently, anodal and cathodal tDCS are simultaneously applied to one motor cortex and the other, respectively (bilateral tDCS) [3, 5, 6, 10, 15–20]. Bilateral tDCS is supposed to combine the effects of anodal and cathodal tDCS and result in larger after-effects compared with unilateral tDCS [3, 10]. However, the advantage of bilateral tDCS is still under debate [15–17, 19] because it has not been fully elucidated how tDCS affects transcallosal inhibition underlying interhemispheric balance between motor cortices.

Studies using transcranial magnetic stimulation (TMS) have demonstrated that transcallosal inhibition is affected by the modulation of intracortical motor circuits in both M1 that project and receive callosal volleys [21–24]. Hence, it is possible that tDCS-induced neuromodulation in the M1 neural circuits affects transcallosal inhibition. Indeed, Lang et al. [25] demonstrated that transcallosal inhibition measured by the duration of ipsilateral silent period (iSP) was increased and decreased by anodal and cathodal tDCS, respectively, that were unilaterally delivered to the motor cortex receiving transcallosal inhibition. However, the robust effects on iSP were not observed after unilateral tDCS given to the motor cortex projecting callosal volleys [25]. These findings may not be in line with the idea that tDCS given to a motor cortex influences the contralateral motor cortex through the modulation of transcallosal pathways. Subsequently, Williams et al. [5] investigated short-interval interhemispheric inhibition (IHI) elicited by paired-pulse TMS and found that IHI was suppressed after the application of bilateral tDCS combined with unimanual motor training. Although the reduction of IHI was accompanied by the decrease of corticospinal excitability in the side of motor cortex projecting callosal volleys, their causal association was not fully elucidated [5].

IHI and iSP are thought to be mediated by different neuronal populations in the transcallosal pathways [26], suggesting the possibility that tDCS does not affect their different neuronal populations in a similar way. Indeed, Gilio et al. [27] demonstrated that 1 Hz repetitive TMS (rTMS) given to the left M1 suppressed IHI from the left M1 to right M1 with minor effects on iSP. Given these physiological backgrounds, we hypothesized that tDCS given at rest would induce polarity-specific after-effects on IHI from the stimulated M1 in which the corticospinal excitability was changed. To examine this hypothesis, we investigated the after-effects of tDCS applied at rest with three different electrode montages (i.e., unilateral anodal, unilateral cathodal, and bilateral). Each montage was intended to elicit either facilitation of right corticospinal excitability, inhibition of left corticospinal excitability, or both. It should be noted that the intended relative change between the left and right corticospinal excitabilities was the same across the three electrode montages, with right greater than left. Before and after each tDCS, single-pulse TMS and paired-pulse TMS were given to the left M1 and right M1 in order to assess the corticospinal excitability and mutual direction of IHI.

Methods

Participants

Participants were sixteen healthy right-handed volunteers (22–34 years old, 3 females). All participants gave their written informed consent to participate in this study. The experimental and consent procedures were approved by the ethical review board of the National Rehabilitation Center for Persons with Disabilities and which was in accordance with the guidelines established in the Declaration of Helsinki. All participants were naïve to the purpose of the experiments.

Recordings

Electromyography (EMG) was recorded from the bilateral first dorsal interosseous (FDI) muscles. Self-adhesive Ag/AgCl electrodes were placed over the muscle belly and the metacarpophalangeal joint. The EMG signals were amplified and filtered (bandwidth, 20–3000 Hz) with a conventional bioamplifier (BIOTOP 6R12, NEC San-ei, Tokyo, Japan). Their digital data were acquired with a sampling rate of 5 kHz with a CED 1401 A/D converter (Cambridge Electronic Design, Cambridge, UK) and stored on a computer for off-line analysis.

TMS

Corticospinal excitability and IHI were investigated by single-pulse and paired-pulse TMS, respectively. TMS was delivered to the left M1 and the right M1 with a figure 8-shaped coil (70-mm diameter) connected to a Magstim 200 (Magstim, Whitland, UK). The stimulus location was determined to be the hot spot where weak stimulation could elicit the largest motor evoked potential (MEP) in the FDI

muscle. The coil was held tangentially over the scalp with the handle pointing backward and 45° lateral away from the midline. The resting motor threshold (RMT) was defined as the minimum stimulus intensity that produced MEPs that were greater than 50 μV in at least 5 out of 10 consecutive trials. For the single-pulse TMS, the intensity of test stimulation (TS) was set at 120% of the RMT. Stimuli were consecutively delivered about every 10 s. Both the left and right hemispheres were examined sequentially with a randomized order across the participants. Fifteen MEPs were obtained at each hemisphere. Paired-pulse TMS was used to elicit IHI both from the left M1 to the right M1 and from the right M1 to the left M1. A suprathreshold conditioning stimulation (CS) with an intensity at 120% of RMT was delivered to M1 on one side 10 ms before a TS was delivered to M1 on the other side. For a few participants, it was impossible to place both coils at the optimal direction due to the size of the coil. Thus, the handle of the coil for the CS was pointed backward and more than 45° away from the midline until both coils did not contact each other. The TS intensity was adjusted so that the peak-to-peak amplitude of the MEP was about 1 mV. The paired-pulse stimulation and TS alone were randomly given every 10 s. Fifteen control MEPs and 15 conditioned MEPs were obtained at each side of tested FDI. For both single-pulse and paired-pulse TMS, if trials showed more than 20 μV of EMG activity in the window of 100 ms before TMS, additional stimuli were given instead of those trials.

tDCS

Direct current stimulation was delivered by a battery-driven constant-current stimulator (Eldith DC-Stimulator, NeuroConn, Ilmenau, Germany) through a pair of rubber electrodes (5 × 5 cm) covered with saline-soaked sponges (5 × 6 cm). We examined three kinds of electrode montages; anodal tDCS over the right M1, cathodal tDCS over the left M1, and bilateral tDCS over the right M1 and left M1. For anodal tDCS, the anode and cathode were positioned on the right M1 (i.e., the hot spot of the left FDI) and the superior edge of the left orbit, respectively (Figure 1A). For cathodal tDCS the anode and cathode were positioned on the superior edge of the right orbit and the left M1 (i.e., the hot spot of the right FDI), respectively (Figure 1B). For bilateral tDCS, the anode and cathode were over the right M1 and left M1, respectively (Figure 1C). The current polarity at each electrode was masked to the participants. 1.5 mA of direct current stimulation was delivered for 15 min. The current was gradually increased and decreased during the first and last 10 s of the stimulation, respectively. Sham-tDCS was conducted for 15 min with the montages of anodal tDCS and bilateral tDCS (Figure 1D, E). The 1.5 mA of direct current stimulation was delivered for first 30 s subsequent to 10 s of current increment.

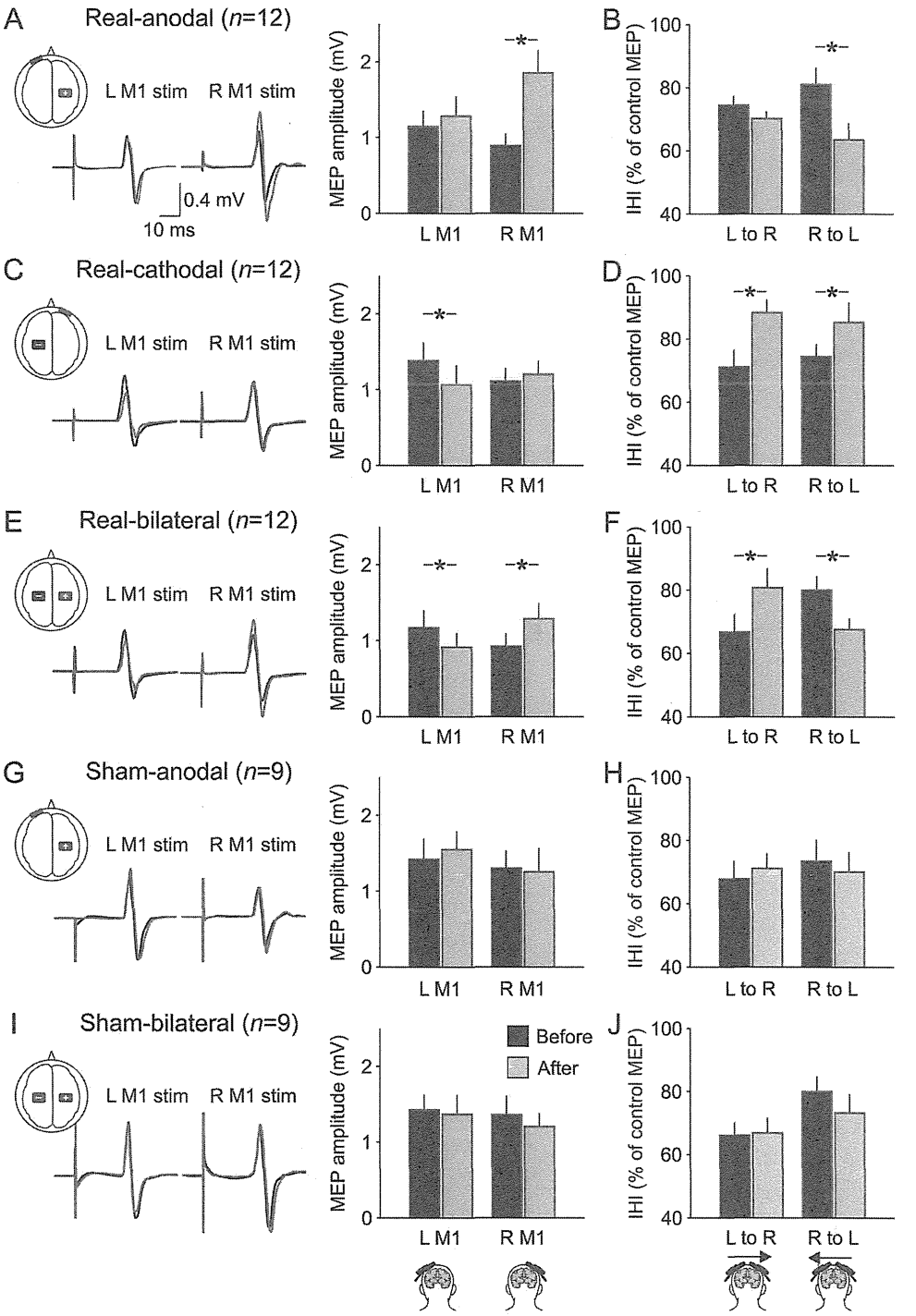

Figure 1. tDCS after-effects on MEPs and IHI. From top to bottom, real-anodal tDCS (A, B), real-cathodal tDCS (C, D), real-bilateral tDCS (E, F), sham-anodal tDCS (G, H), and sham-bilateral tDCS (I, J). The left and right sides of the traces are MEPs that are elicited by single-pulse TMS over the left M1 and right M1, respectively. The black and gray lines indicate MEPs that were elicited before and after DCS, respectively. The left bar graphs (A, C, E, G, J) show the average data of MEP of all participants. The sets of the left- and the right-sided columns represent MEP amplitude elicited by left (L) M1 stimulation and right (R) M1 stimulation, respectively. The rights bar graphs (B, D, F, H, J) show the average data of IHI of all participants.

IHI was expressed as the ratio of the conditioned MEP amplitude normalized by the control MEP amplitude (i.e., larger value indicates less IHI). The sets of the left- and right-sided columns represent IHI from the left M1 to the right one (L to R) and that from the right M1 to the left one (R to L), respectively. The black and gray columns represent before and after tDCS, respectively. Error bas show standard error of means. The asterisks indicate a significant difference; * $p<0.05$.

doi:10.1371/journal.pone.0114244.g001

Experimental procedures

The experiments were composed of real-tDCS and sham-tDCS sessions. 12 participants joined the real-tDCS session and 9 participants joined the sham-tDCS session. 5 out of 16 participants were involved in both sessions; three of them participated in the real-tDCS session first and two of them participated in the sham-tDCS session first. Each kind of electrode montage was tested on a different day. At least 3 weeks were interleaved across the experimental days. At each tDCS session, the order of the electrode montages was randomized across participants. In the experiments, the participants sat comfortably on a reclining chair with their shoulders and elbows semi-flexed. Both of their hands were placed on the table with palms downward. Before the tDCS application, RMT was measured in both M1. Then, the single-pulse and paired-pulse TMS protocols were conducted. After these baseline measurements were made, real- or sham-tDCS with an electrode montage was given for 15 min. After tDCS application, the same measurements were conducted on each side of M1.

Data analysis

For the evaluation of corticospinal excitability, the peak-to-peak amplitudes of the MEPs elicited by single-pulse TMS were measured in the window 18–50 after the TMS trigger. The extent of after-effects was expressed as the ratio of the MEP amplitude obtained after tDCS to the baseline MEP amplitude obtained before tDCS. In order to evaluate IHI, the amplitude of the conditioned MEPs elicited by paired-pulse stimulation were normalized by the amplitude of the control MEPs evoked by TS alone. Trials with more than 20 μV of peak-to-peak amplitude in background EMG activity for 100 ms pre-stimulus period were discarded from the analysis. For the statistical analysis, a three-way analysis of variance (ANOVA) with repeated measures was performed with factors of time (before and after tDCS), tDCS type (real-anodal, real-cathodal, real-bilateral, sham-anodal, sham-bilateral), and TS side (left and right M1). In case a significant interaction between three factors was obtained, appropriate follow-up two-way ANOVA was conducted to examine the interaction of time and TS side factors at each tDCS type. In order to compare the magnitude of after-effects across conditions, one-way ANOVA with repeated measures was conducted with factor of tDCS type at each TS side. For the comparison of baseline level in each measurement, two-way ANOVA with repeated measures was performed with factors of tDCS type and TS side. *Post-hoc* comparisons were conducted by Tukey's test.

According to the findings in the previous studies [12, 16], we expected that real-tDCS induced the polarity-specific modulation in the M1 underneath the active electrode. Thus, we anticipated that real-tDCS influenced the excitability of callosal neurons in the same M1. Therefore, to examine the relationship between the after-effects on MEP amplitude and IHI, we also conducted Pearson correlation analysis in the real-tDCS after-effects between MEP amplitude and IHI. *P* values less than 0.05 were recognized as statistically significant in all analyses. Group data are presented as the mean ± standard deviation in the text.

Results

RMT, MEP

RMT was different across TS sides ($F_{1,49}=5.53$, $p=0.02$). TMS given to the left M1 showed slightly lower RMT than the right M1 (Table 1). However, tDCS did not affect RMT ($F_{1,49}=0.43$, $p=0.51$) regardless of tDCS type ($F_{4,49}=0.70$, $p=0.59$). Three-way ANOVA did not show any significant interactions (time × tDCS type, $F_{4,49}=0.07$, $p=0.99$; time × TS side, $F_{1,49}=0.26$, $p=0.62$; tDCS type × TS side, $F_{4,49}=0.24$, $p=0.92$; time × tDCS type × TS side, $F_{4,49}=1.00$, $p=0.42$).

Figure 1A illustrates representative example of MEPs elicited before and after tDCS. Consistent with the findings in the previous studies [12, 16], facilitation and inhibition were observed in the MEPs elicited by single-pulse TMS over the M1 under the anode and the cathode, respectively. Three-way ANOVA revealed significant interactions of time and tDCS type and TS side ($F_{4,49}=4.39$, $p=0.004$) on MEP amplitude, indicating that the interaction of time and TS side was dependent on the tDCS type. Then, we performed follow-up two-way ANOVA for each tDCS type. Regardless of electrode montage, real-tDCS showed significant interaction of time and TS side (real-anodal, $F_{1,11}=8.32$, $p=0.02$; real-cathodal, $F_{1,11}=5.76$, $p=0.04$; real-bilateral, $F_{1,11}=23.53$, $p<0.001$), indicating that all electrode montage had tDCS after-effect on MEP amplitude such that their tDCS after-effects were different depending on the TS side. *Post-hoc* analysis revealed that after real-anodal tDCS over the right M1, the MEP elicited from the right M1 was increased (232.0 ± 144.7%, $p<0.001$) and the MEP elicited from the left M1 was unchanged (111.1 ± 41.7%, $p=0.54$) compared with the baseline (Figure 1A). After real-cathodal tDCS over the left M1, the MEP elicited from the left M1 was decreased (76.2 ± 27.6%, $p=0.01$) and the MEP elicited from the right M1 was unchanged (109.0 ± 36.5%, $p=0.45$, Figure 1C). After real-bilateral tDCS (anode over the right M1, cathode over the left M1), the MEP elicited from the right M1 was increased (157.6 ± 68.2%, $p<0.001$) and the MEP elicited from the left M1 was decreased (75.4 ± 28.3%, $p=0.01$, Figure 1E). In contrast to real-tDCS, nether of sham-tDCS showed significant main effect of time (sham-anodal, $F_{1,8}=0.38$, $p=0.55$; sham-bilateral, $F_{1,8}=1.36$, $p=0.28$) or TS side (sham-anodal, $F_{1,8}=1.17$, $p=0.31$; sham-bilateral, $F_{1,8}=0.66$, $p=0.44$), or their interaction (sham-anodal, $F_{1,8}=2.68$, $p=0.14$; sham-bilateral, $F_{1,8}=0.05$, $p=0.84$, Figure 1G, I). Two-way ANOVA revealed that baseline level of MEP amplitude before tDCS was not

Table 1. Resting motor threshold (% maximal stimulator output).

		Real-tDCS (n=12)			Sham-tDCS (n=9)	
		Anodal	Cathodal	Bilateral	Anodal	Bilateral
Left M1	Before	43.8±6.1	44.7±6.9	43.8±6.8	46.1±7.6	46.6±7.5
	After	43.5±5.5	45.0±7.8	44.4±6.5	46.0±7.6	46.0±7.6
Right M1	Before	44.7±6.0	46.8±9.8	45.7±8.1	48.3±7.6	48.4±5.6
	After	44.2±6.5	46.1±10.7	44.7±8.9	48.6±7.0	48.9±6.7

Values are mean ± standard deviation.

doi:10.1371/journal.pone.0114244.t001

different across tDCS types ($F_{4,49}$=0.96, p=0.44) or TS sides ($F_{1,49}$=3.79, p=0.06) with no interaction of their factors ($F_{4,49}$=0.07, p=0.99).

To sum up, facilitation and inhibition were observed in the MEPs elicited from the M1 under the anode and the cathode, respectively. With real-anodal and real-cathodal tDCS, the MEP elicited from the unstimulated M1 was unchanged. The magnitude of after-effects was not different across the conditions that showed significant facilitation (real-anodal 232.0±144.7%, real-bilateral 157.6±68.2%, p=0.20) or inhibition (real-cathodal 76.2±27.6%, real-bilateral 75.4±28.3%, p=0.99).

IHI

Both before and after tDCS, IHI was examined both from the left M1 to the right M1 and from the right M1 to the left M1. By adjusting the TS intensity to elicit a 1 mV MEP, the amplitude of the control MEP was not different across conditions. Three-way ANOVA revealed significance of neither main effect of time ($F_{1,49}$=0.07, p=0.80), tDCS type ($F_{4,49}$=0.1.74, p=0.16), TS side ($F_{1,49}$=0.33, p=0.57), nor their interactions (time × tDCS type, $F_{4,49}$=0.76, p=0.59; time × TS side, $F_{1,49}$=0.10, p=0.76; tDCS type × TS side, $F_{4,49}$=0.40, p=0.81; time × tDCS type × TS side, $F_{4,49}$=0.24, p=0.91).

The three-way repeated measures ANOVA revealed significant interaction of time and tDCS type and TS side ($F_{4,49}$=2.64, p=0.04) on IHI, indicating that the interaction of time and TS side was dependent on the tDCS type. Then, we performed follow-up two-way ANOVA for each tDCS type. Real-anodal and real-bilateral tDCS showed significant interaction of time and TS side (real-anodal, $F_{1,11}$=8.36, p=0.02; real-bilateral, $F_{1,11}$=20.08, p<0.001). On the other hand, real-cathodal tDCS had only main effect of time ($F_{1,8}$=9.42, p=0.01) but not main effect of TS side ($F_{1,8}$=0.001, p=0.98) or interaction of time and TS side ($F_{1,8}$=1.78, p=0.21). That is, in the real-tDCS session, all electrode montages had tDCS after-effect on IHI. The tDCS after-effect was different depending on the TS side (i.e., direction of IHI) after real-anodal and real-bilateral tDCS. On the other hand, the after-effect of real-cathodal tDCS was independent of TS side. *Post-hoc* analysis demonstrated that after real-anodal tDCS over the right M1, IHI from the right M1 to the left M1 was significantly increased compared with baseline

($p<0.001$). However, IHI from the left M1 to the right M1 was unchanged ($p=0.16$, Figure 1B). After real-cathodal tDCS over the left M1, a reduction in IHI magnitude was observed both from the left M1 to the right M1 and from the right M1 to the left M1 ($p=0.01$, Figure 1D). After real-bilateral tDCS (anode over the right M1, cathode over the left M1), IHI from the left M1 to the right M1 was decreased compared with baseline ($p=0.001$). In contrast, IHI from the right M1 to the left M1 was increased compared with baseline ($p=0.003$; Figure 1F). Again, neither of sham-tDCS affected IHI (Figure 1H, J). Two-way repeated measures ANOVA did not show any significant effect of time (sham-anodal, $F_{1,8}=0.0003$, $p=0.99$; sham-bilateral, $F_{1,8}=0.28$, $p=0.61$), TS side (sham-anodal, $F_{1,8}=0.11$, $p=0.75$; sham-bilateral, $F_{1,8}=5.10$, $p=0.06$), or their interaction (sham-anodal, $F_{1,8}=0.62$, $p=0.45$; sham-bilateral, $F_{1,8}=1.68$, $p=0.23$). Baseline level of IHI before tDCS was generally larger from the left M1 to the right M1 than the opposite direction. Two-way repeated measures ANOVA showed significant effect of TS side on the baseline level of IHI ($F_{1,49}=10.78$, $p=0.002$), but not main effect of tDCS type ($F_{4,49}=0.40$, $p=0.81$) or interaction of tDCS type and TS side ($F_{4,49}=0.67$, $p=0.62$), indicating that although an asymmetry of IHI was observed across IHI directions, the baselines of IHI on each direction was similar level across tDCS types.

In summary, IHI from the M1 under the anode was increased. In contrast, IHI from the M1 under the cathode was decreased. IHI from the unstimulated M1 showed a decrease after cathodal tDCS, but it was unchanged after anodal tDCS. Finally, we tested the correlation of tDCS after-effects between MEP amplitude and IHI. However, we did not find any significant correlations between the modulations of MEP amplitude and IHI regardless of TS side (Table 2).

Discussion

The present study demonstrated that tDCS produced polarity-specific after-effects on IHI from the stimulated M1 at which the corticospinal excitability was changed. Regardless of unilateral or bilateral tDCS, IHI was generally increased from the M1 at which the corticospinal excitability was increased and decreased from the M1 at which the corticospinal excitability was decreased. Bilateral tDCS simultaneously produced the opposite directional modulation in IHI from the left to the right M1 and in IHI from the right to the left M1 in addition to the bidirectional corticospinal modulation. Although unilateral anodal tDCS did not affect the corticospinal excitability at the side of unstimulated hemisphere or IHI from the M1 on that unstimulated hemisphere, unilateral cathodal tDCS suppressed IHI from the M1 on the unstimulated hemisphere even though the corticospinal excitability was unchanged at the unstimulated side.

In most cases, the modulations of IHI were parallel to the modulations of corticospinal excitability at the side sending callosal volleys. Thus, it is likely that the tDCS after-effects on IHI are relevant with the excitability change in the motor cortex sending callosal volleys. However, we did not observe any significant